Applied Water Science (2022) 12:190
https://doi.org/10.1007/s13201-022-01711-6

ORIGINAL ARTICLE

Wetland landscape pattern evolution and prediction in the Yellow River Delta

Ke Zhou[1]

Received: 9 April 2022 / Accepted: 1 June 2022 / Published online: 28 June 2022

Abstract

Starting from the overall pattern of wetland evolution in the Yellow River Delta, the combination of CA–Markov model and MLP model is studied. Based on the low-medium resolution Landsat data and the field survey data, the evolution trend of wetland landscape pattern in the Yellow River Delta is simulated and predicted by using the proposed models. Taking high resolution (2 m) data in 2016 as the precision verification, the model simulation results are validated. The results show that the area of natural wetlands in the Delta was decreased from 2593.63 km^2 in 1976 to 1639.60 km^2 in 2016, a total area of 954.03 km^2wasreduced. According to the model simulation, the natural wetland area in 2026 is predicted to be 1252.7 km^2, the constructed wetland area will be 1265.0 km^2, and the non-wetland area will be 924.5 km^2. The constructed wetland in the Yellow River Delta is increasing and spreading into the sea, but the area of natural wetland has been decreasing. If this trend be developed, the national natural wetland conservation target would not be realized. The results are of great significance to the wetland development planning, management and protection in the Yellow River Delta.

Keywords Wetland · Landscape pattern · Evolution and prediction · The Yellow River Delta

Introduction

The change and evolution trend of wetland landscape are directly related to the survival and development of human beings (Davidson 2014). In recent years, a lot of researchers studied the wetland landscape patterns (Chang et al. 2014). In 2004, Walter et al. conducted a study on dynamic variation of wetland landscape pattern by using supervised classification and visual identification methods and remote sensing images of the Yellow River Delta, to find the degree of wetland landscape variation and the driving factors affecting the wetland change in the region (Walter et al. 2004). In 2015, Dronova et al. used the data (1973 ~ 2013) to analyze the wetland evolution and related driving factors by using the method of visual identification (Dronova et al. 2015). In 2016, Liu JF. et al. used the TM image data (1989 ~ 2014) to classify and calculate the wetland index by using artificial visual identification, which reflects the intensity of human activities. The impact of human activities on the Yellow River delta was analyzed from a quantitative point (Liu et al. 2016).

From the viewpoint of data, with the rapid development of remote sensing technology, in recent years, high resolution series and aerial photography data have become the mainstream of wetland dynamic monitoring Fu et al. 2013, Mui et al. 2015). Klemas studied the high resolution images, low-medium resolution images and aerial photograph data to find that the long-term and short-term change trend of wetland vegetation and hydrology can be effectively determined by conjunctive use of satellite images, aerial images and ground observation survey data (Klemas 2013). Data conjunctive use has become the mainstream trend of wetland information collection in recent years (Dong et al. 2016).

From the perspective of classification method, the traditional classification method is based on supervised and unsupervised classification, which only takes into account the spectral information of images (Escorihuel et al. 2016). In 2009, Frohn et al. put forward a method of wetland information extraction which combines between regional and stratification information to improve the accuracy of traditional classification method, the precision was increased from 85 to 91.97%, which greatly improves the accuracy of wetland classification (Frohn et al. 2009). In 2018, by using

✉ Ke Zhou
zhouke828282@163.com

[1] North China University of Water Resources and Electric Power, Jinshui Road 136, Zhengzhou 450046, Henan, China

the Landsat satellite images and taking the typical wetland in China as the study area, Mao et al. used the objective-oriented method to classify the wetland landscape. The studied results were compared with the corresponding classification results obtained by using the maximum likelihood method, artificial neural network and support vector machine method to prove that the objective-oriented method has a higher classification accuracy (Mao et al. 2018). In 2013, Liu Y et al. used regional classification method to identify wetland landscape in the eastern coastal China (Liu et al. 2013). In 2017, Congru MU, et al. used the remote sensing images of the Yellow River Delta from the 6 phases of Landsat series to extract the information of human activities. Base on the objective-oriented decision tree algorithm, the landscape patterns were classified and the changing rate, transfer types and other characteristics were analyzed (Congru et al. 2000).

In the above study findings, the most of classification methods are manual vector and pixel-based methods. The manual vector method includes many artificial interference factors, high cost and heavy workload (Mishra et al. 2014, Ozesmi et al. 2002). The traditional pixel-based classification method would causes large fragmentation and great differentiation. The minimum unit of processing image in the objective-oriented method is a separate pixel image rather than the entire objective entity, which would cause large errors in the final results.

Therefore, in order to overcome the shortcomings in the above relevant study findings, this paper proposed wetland simulation and prediction theoretical methods including CA–Markov model, multi-layer perception(MLP) model, and combination model of a CA–Markov model with MLP. Taking high resolution (2 m) data in 2016 as the precision verification, the model simulation results are validated.

Starting from the entire evolution pattern of wetland in the Yellow River estuary, and using low-medium resolution Landsat series of data, the evolution trend of wetland landscape pattern in the Yellow River Delta was simulated and predicted, which is of great significance to the development planning, management and protection of wetland in the Yellow River Delta.

Data and methods

Data source

The data from the official website of the United States Geological Survey (USGS) were selected as the basic data for wetland classification, including Landsat2 MSS (2 June 1976), Landsat5TM (20 May 1986), Landsat5TM (20 September1996), Landsat5TM (2 October2006), Landsat 8 TM (26 August2016). The wetland classification data in the Yellow River Delta, field survey data in 2017, and high resolution (2 m) data in 2016 were used as auxiliary data for accuracy verification. The vector files include vector boundary data of modern Yellow River Delta, road traffic data, statistical yearbook of Dongying City from 2000 to 2017, Dongying City history records and other statistical data (Dongying Municipal Government 2019), Dongying City "13th Five-Year Plan "for Modern Agricultural Development (Dongying Municipal Government 2016). The data source and description are shown in Table 1.

Methods

CA–markov model

CA model The cellular automation (CA) was proposed by Neumann and Ulan in 1940 s (Keddy 2000). The principle is to predict the state transformation in the next time period according to the specific conversion rules starting from the current cell state and the neighborhood state.

CA model is a dynamic model with temporal-spatial computational ability and spatial modeling ability, which is characterized by discrete time, space and state, as shown in Eq. (1).

$$S_{(t+1)} = f(S_{(t)}, N) \tag{1}$$

where S is a set of finite and discrete states, N is the neighborhood of the cell, f is the cell state transformation rule in the local space.

CA model consists of four important parts, i.e., cell (wetland pixel), state (wetland landscape types), neighborhood (a pixel adjacent to several surrounding pixels), and conversion rule (wetland conversion rule to other types of wetland pixels). CA model has a strong ability to simulate spatial information, but has low ability to capture large amount of data. The

Table 1 The data source and description

Files	Time	Resolution	Cloud (%)	Function
Landsat 2 MSS	2, June,1976	78 m	0	Basic data
Landsat 5 TM	2,May, 1980	30 m	0	Basic data
Landsat 5 TM	2,Sept. 1996	30 m	0	Basic data
Landsat 5 TM	2, Oct. 2006	30 m	0.36	Basic data
Landsat 8 OLI	26, Aug.2016	30 m	0	Basic data
ZY3705-464,452	25, Jun. 2016	2 m	0	Verification
GF3705-752,914	10, Aug.2016	2 m	0	Verification
GF3705-542,202	25, Apr. 2016	1 m	0	Verification
ZY3705-464,453	25, Jun. 2016	2 m	0	Verification

combination of CA with Markov model can improve the space and quantity of simulation results.

Markov model Markov model is used as the basis of CA-Markov and MLP model combination (Olmedo et al. 2015). A Markov transfer matrix was constructed using the classification results in 1996 and 2006. The model matrix P_{ij} can be calculated using Eq. (2).

$$P_{ij} = \begin{bmatrix} P_{11} & P_{12} & \cdots & P_{1n} \\ P_{21} & P_{22} & \cdots & P_{2n} \\ \vdots & \vdots & \vdots & \vdots \\ P_{n1} & P_{n2} & \cdots & P_{nn} \end{bmatrix} \quad (2)$$

where the values of the diagonal $P_{11,}$ $P_{22}\ldots P_{nn}$ in the matrix represent the unchanged transfer elements from T_0 to $T_{1.}$ The values of off-diagonal $P_{12,}$ $P_{21}\ldots P_{1n}$, P_{n1}in the matrix represent the changed transfer elements from T_0 to T_1.

In this paper, the cell iterations were set for 10 times. The verification was made through comparison of the simulated results with the measured results in 2016. In CA-Markov simulation, parameters setting could affect the accuracy of simulation results, see Table 2. When the value equals to 0, the classification accuracy of the representative images can reach 100%, which is similar to the transfer matrix automatically generated by the MLP model. When the value equals to 0.15, the classification accuracy of representative images can generally reach more than 85%. The quantitative results of the simulation are affected by the generation of transfer probability matrix.

Multi-layer perception(MLP)model

MLP neural network model includes input layer, output layer and multiple hidden layers, which is a multi-layer forward feed neural network based on BP algorithm trained (Williams et al. 1995). Among different neural network structures, MLP neural network is the simplest, and easy to implement, and has strong nonlinear mapping ability (Lin et al. 2007). In general, the number of hidden neurons in MLP can be determined by the following two empirical formulas.

$$N_H = \sqrt{N_1 + N_O + \alpha} \quad (3)$$

Table 2 Proportional error parameter settings

Process	Proportional error	Quantitative error
CA-Markov	0	0.1451
CA-Markov	0.15	0.1139

$$N_n = \frac{N_{\text{training}}}{\alpha(N_1 + N_O)} \quad (4)$$

where N_H is th number of hidden neurons in MLP, N_1 is the number of input layer, N_o is the number of the output layer, α is an integer with values 1–10, N_{training} is the number of training samples.

The combination of MLP with CA-Markov

CA–Markov model has better simulation results on quantity, and MLP model has better simulation results on space location. In order to make use of the different advantages of the two models, in this paper, the CA–Markov model matrix was combined with the MLP model. The final quantity error is 0.1135, and location error is 0.2143. Therefore, the combination of CA–Markov model and the MLP model can improve the accuracy of spatial and temporal variation prediction of wetland landscape pattern.

Accuracy verification

The sample matrix was used as an accuracy method to verify the model accuracy in this paper. 20 accuracy verification points are randomly taken for each kind of landform types. The verified results show that the comprehensive accuracy is 83.75% in 1976, the accuracy is 82.30% in 1986, the accuracy is 81.79% in 1996, the accuracy is 79.67% in 2006, and the accuracy is 81.33% in 2016. The accuracy verification matrix in 2016 is shown as Table 3.

Case study

Background

The Yellow River Delta lies in the Bohai Sea to the north and Laizhou Bay to the east. The geographical coordinates spans from 117°31′E ~ 119°18°31′E to 36°55°31′N ~ 38°16°31′N. The climate in the area belongs to the continental semi-humid monsoon climate, with the annual average temperature from 11.7 to 12.6 ℃, and annual average precipitation from 530 to 630 mm, of which 70% are concentrated in summer. The annual evaporation capacity is 1900 ~ 2400 mm.

The Delta formation comes from the large amount of sediment from the Yellow River. The topography of the Yellow River Delta is slightly fluctuated, relatively higher in the west and south, and lower in the east and north. The wobble of the Yellow River's course has adversely affected the ecological protection and environment of the Yellow River Delta and severely restricted economic and social development in the Yellow River Delta. The Yellow River Delta

Table 3 Accuracy verification matrix in 2016

Elements	1	2	3	4	5	6	7	8	9	10	11	12	13	14	15	KIA
1 natural land	17	0	0	2	2	0	0	0	0	0	0	0	0	1	0	0.84
2 construction	0	16	0	1	0	0	0	0	0	0	0	1	0	0	0	0.79
3 reed land	0	2	16	1	2	1	2	2	3	1	0	0	1	1	0	0.78
4 industrial	0	0	0	15	0	0	0	0	0	0	0	0	0	0	0	0.74
5 beach	2	0	0	0	16	0	0	2	0	0	0	0	0	0	0	0.79
6 ponds	1	1	0	0	0	16	2	0	0	0	0	0	0	0	0	0.79
7 aqua-culture	0	0	0	0	0	0	16	0	0	0	2	0	0	0	0	0.79
8 suaeda salsa	0	0	0	0	0	0	0	15	0	0	0	0	0	1	0	0.74
9 dry land	0	1	0	0	0	1	0	0	15	1	0	4	2	0	0	0.73
10 waste land	0	0	0	1	0	1	0	0	0	17	0	0	0	0	0	0.84
11 salt land	0	0	0	0	0	0	0	0	0	0	17	0	0	0	0	0.84
12 paddy land	0	0	1	0	0	1	0	0	1	1	1	15	1	0	0	0.73
13 forestry	0	0	0	0	0	0	0	0	0	0	0	0	16	0	0	0.79
14 interleaved rice grass	0	0	3	0	0	0	1	0	0	0	0	0	0	17	0	0.84
15 garden land	0	0	0	0	0	0	0	0	1	0	0	0	0	0	20	1.00

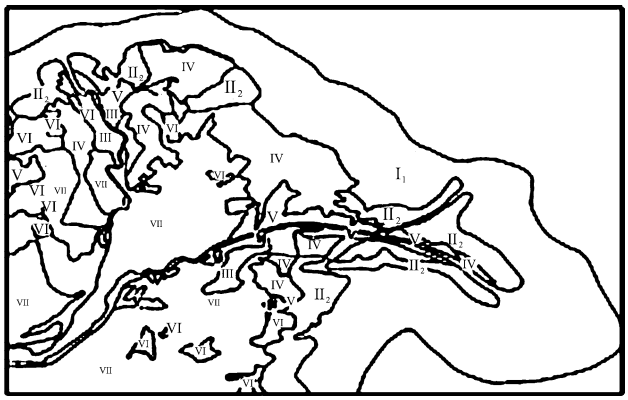

Fig.1 Distribution of wetland in Yellow River Delta

is rich in sediment resources and has a great potential for economic development (Chen 2019).

In 1994, the Yellow River Delta Wetland Nature Reserve was listed as one of the 16 important natural reserves in the world. In 2013, the Yellow River Delta was selected in the list of International Importance Wetlands by the Secretariat of the Wetlands Convention. The research area of this paper focus on the present fan-shaped area of the Yellow River Delta, which takes Yuwa of Kenli county as an axis point, from Tiaohekou to Song Chunrong, the total area is 5400 km^2, Fig. 1.

(I. Natural wetland; I_1. Sub-tidal wetland, II_2. Inter-tidal wetland,II. Estuary wetland, III. River wetland,IV. Marshland, V. Wet-meadow,VI. Artificial wetland, VII. Farmland.)

Dynamic transfer of wetland types

From the Yellow River Delta wetland landscape transfer matrix model, we can see the temporal- spatial variation of wetland landscape types, see Table 4.

Arc Gis 10.2 software was used in this paper to complete the temporal-spatial dynamic analysis of wetlands from 1976 to 2016. According to statistics, the change matrix of wetland transfer can be obtained.

The transfer matrix from 1976 to 2016 shows that most of the natural wetland has been transferred to constructed

Table 4 Landscape transfer matrix

Time	Landscape types	T_2					
		A_1	A_2	A_3	–	A_{n-1}	A_n
T_1	A_1	a_{11}	a_{12}	a_{13}	–	a_{1n-1}	a_{1n}
	A_2	a_{21}	a_{22}	a_{23}	–	a_{2n-1}	a_{2n}
	A_3	a_{31}	a_{32}	a_{33}	–	a_{3n-1}	a_{3n}
	–	–	–	–	–	–	–
	A_{n-1}	a_{n-11}	a_{n-12}	a_{n-13}	–	a_{n-1n-1}	a_{n-1n}
	A_n	a_{n1}	a_{n2}	a_{n3}	–	a_{nn-1}	a_{nn}

Note T_1 refers to the first time period, T_2 refers to the second time period, A_1-A_n refers to the landscape types, a_{nn} refers to the landscape area transferred from types n in period T_1 to types n in period T_2

wetland and non-wetland over the past 40 years, in which, 31.34% of the suaeda glauca bunge was transferred toponds,24.70% of the suaeda glauca bunge was transferred to salt field,15.42% of the suaeda glauca bunge was transferred to aqua-culture ponds,4.13% of tidal beach was transferred to salt field,6.34% of tidal beach was transferred to aqua-culture ponds,13.22% of tidal beach was transferred to ponds, 5.96% of the tidal beach was converted to industrial and mining land,24.71% of the reeds land was transferred to dry land, and 2.79% of the suaeda glauca bunge was converted into the dry land. The constructed wetland is mainly transferred to non-wetland, in which, 21.27% of the ponds was transferred to dry land. 1.55% of ponds was transferred to architecture land. In the transformation of non-wetland, 40.11% of the waste land was converted to dry land, and 30.52% of the forest land was transferred to dry land. Therefore, it shows that the dynamic change has been happened during 40 years.

Analysis on wetland area change

It can be seen from Fig. 2 that the total area of natural wetlands in the region show a continuous downward trend from 1976 to 2016.

From 1976 to 2016, natural wetland area was decreased from 2593.63 to 1639.60 km^2, which totally reduced 954.03 km^2. During 40 years, reeds area showed an increasing tendency first and then decreasing, a total of 511.47 km^2 was reduced. The constructed wetland area showed an increasing trend, which increased from 1.13 km^2 in 1976 to 852.19 km^2in 2016, a total of 851.06 km^2 increased. Ponds area was maintained increasing trend. During 40 years, a total of 298.24 km^2 ponds area was increased. Salt field area was increased by 92.95 km^2. Aqua-culture pond area was increased by 126.61 km^2. Paddy land was increased by 333.25 km^2, which was mainly concentrated between 2006 and 2016, a total of 293.76 km^2Paddy land was increased over a decade. In non-wetland, dry land was maintained increasing trend, a total of 356.15 km^2 dry land was increased.

The area changes of different wetland landscape area over the different periods from 1976 to 2016 are shown in Table 5

Analysis on wetland landscape index variation

The quantitative landscape pattern can be described and analyzed by the changing trend of landscape index. Considering the granularity and scale effects between landscape indexes, 10 indexes were selected to carry out analysis on landscape variation, i.e., the number of patches(NP), Shannon diversity index(SHDI), patches density index(PDI), patches aggregated index(PAI), landscape shape index(LSI), perimeter-area fractal index(PAFI), landscape fragmentation index(LFI), patches richness index (PRI), Shannon evenness index(SHEI), and patches spreading index(PSI). The calculated results are shown in Table 6.

It can be seen from Table 6 that during 40 years, patches richness index (PRI) show increasing trend, which means that species diversity was increased in the study area. The increase in species diversity also led to a significant increase in the number of patches (NP). Therefore, the patches density index (PDI) and the patches number maintain the increasing trend. Landscape shape index (LSI) shows periodically an upward trend, which shows the complex landscape shape variation. The main reason is due to the increase of landscape types and the interference from human activities. Shannon diversity index (SHDI) and Shannon evenness index (SHEI) experience the increasing trend, which shows that the landscape types in the study area are increased and the distribution is more uniform. Landscape fragmentation index (LFI) shows the increasing trend, which is closely related to human activities, and more large areas of reeds and waste land were developed to small dry fields, breeding ponds and salt fields by human activities. Patches spreading

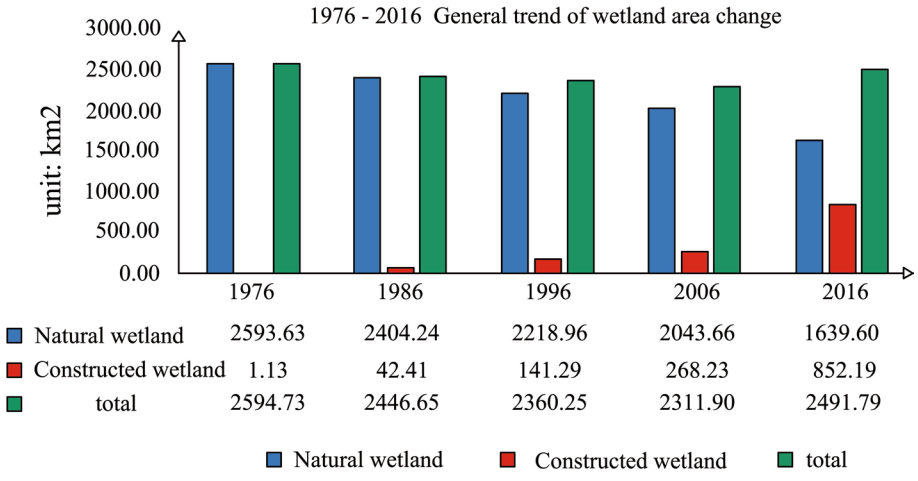

Fig.2 General change trend of wetland area from 1976 to 2016

Table 5 Area changes of wetland landscape in different periods (km.^{2})

Types	1976–1986	1986–1996	1996–2006	2006–2016	1976–2016
1 Interleaved rice grass	0.00	3.45	1.05	20.71	25.21
2 Suaeda glauca bunge	10.14	− 11.61	5.39	− 22.30	− 18.38
3 Reeds land	11.51	− 115.4	− 173.99	− 233.6	− 511.47
4 Beach land	− 1.00	63.63	− 56.46	− 240.51	− 234.34
5 Natural water	− 210.04	− 125.36	48.71	71.64	− 215.05
6 Ponds	2.57	48.54	44.12	203.01	298.24
7 Paddy land	32.23	4.85	2.43	293.74	333.25
8 Salt land	1.60	10.37	79.30	1.68	92.95
9 Aqua-culture	4.87	35.13	1.09	85.52	126.61
10 Industrial land	27.45	20.44	27.25	3.88	79.02
11 Dry land	271.22	225.11	47.54	− 187.71	356.15
12 Architecture	13.42	5.91	19.63	37.83	76.79
13 Forestry	22.66	12.05	0.43	47.72	82.86
14 Waste land	− 186.64	− 177.11	− 51.59	− 83.98	− 499.31
15 Garden land	0.00	0.00	5.09	2.37	7.45

Table 6 Landscape index changing trend during 40 years

Time period	PRI	PDI	LSI	PAFI	LFI	SHDI	SHEI	NP	PSI	PAI
1976–1986	8.0	0.12	12.25	1.33	7.02	1.58	0.76	417.0	60.20	98.93
1986–1996	13.0	0.21	21.03	1.37	8.19	1.76	0.69	733.0	63.18	98.05
1996–2006	14.0	0.30	18.47	1.27	9.19	1.88	0.71	1028.0	62.27	98.33
2006–2016	15.0	0.42	23.01	1.30	10.13	1.99	0.74	1451.0	60.67	97.87
1976–2016	15.0	0.78	35.03	1.31	11.06	2.19	0.81	2701.0	55.84	96.65

index (PSI) has the decreasing trend, which shows that the landscape elements are densely distributed and patches are more fragmented. Patches aggregated index (PAI) has decreasing trend, which shows that the patches is scattered and tends to be broken.

According to the above analysis, the wetland landscape in the Yellow River estuary region generally tends to be transferred from the simplicity to the complexity.

Discussion

Analysis on wetland transfer accuracy

It can be seen from the simulation results that the CA–Markov model can obtain better results in quantity and the MLP model can achieve better results in space. On the whole, the combination of two models can get better results both in quantity and space. Therefore, the combination of CA-Markov and MLP model was used in this paper to obtain satisfactory results.

The simulation results show that the natural wetland area is estimated to be 1252.6857 km^2, the constructed wetland area will reach to 1265.0049 km^2 and the non-wetland area will reach to 924.5070 km^2 in 2026.

After MLP model training, the transfer accuracy of non-wetland to the constructed wetland is 64.14%, the transfer accuracy of non-wetland to natural wetland is 56.30%, the transfer accuracy of the constructed wetland to non-wetland is 70.39%, the transfer accuracy of the constructed wetland to natural wetland is 68.96%, the transfer accuracy of natural wetland to non-wetland is 87.56%, and the transfer accuracy of natural wetland to the constructed wetland is 85.80%.

It can also be seen that according to the change trend from 2006 to 2016, the area of constructed wetland in the Yellow River Delta is still increasing and spreading to the sea, but the area of natural wetland is decreasing.

Analysis on the changing trend under the impact of human activities

Based on the landscape transfer matrix, the concept of human activity impact index (HAII) is put forward to accurately measure the intensity of human activity, as Eq. (5)

$$\mathrm{HAII} = \Delta a / \Delta A \tag{5}$$

where Δa is the area change induced by human activity, ΔA is the total area change.

The transformation from natural wetland to paddy field, aqua-culture pond, salt field, ponds, dry field, architecture land, industrial land or from constructed wetland to dry field, architecture land and industrial land are occurred and have the features of periodical occurrence due to human disturbance, but the transformation from non-wetland to constructed wetland shows the developing trend in the future. The statistics of transferred area in 5 time periods are listed in Table 7.

It can be seen from Table 7 that the transferred area from natural wetland to constructed wetland and non-wetland account for the largest proportion of the total transferred area due to human activities.

It can also be seen from the human activity impact ratio that the impact of human activities on wetland landscape change has the increasing trend.

The area transfer from natural wetland to different types of constructed wetland and non-wetland in five stages are shown in Table 8.

It can be seen from Table 8 that the main human activity influencing factors were farmland reclamation from 1976 to 2006, and the main human activity influencing factors were pond and reservoir construction from 2006 to 2016. From 1976 to 2016, farmland reclamation is the main human activity, and the construction of water pond and reservoir, paddy field and aqua-culture ranks the second.

Analysis on spatial change trend

The sub-regional impact of human activities during different time periods were evaluated using the proposed models. The calculation methods are as follows,

$$\mathrm{HAILS} = \frac{S_{\mathrm{CLE}}}{S} \times 100\% \tag{6}$$

$$S_{\mathrm{CLE}} = \sum_{i=1}^{n} (SL_i.CI_i) \tag{7}$$

where HAILS represents human activity intensity on the terrestrial surface, S_{CLE} is the equivalent area of constructed wetland, km^2, Sis total wetland area in the region, km^2, SL_i is the *i*th wetland landscape area, km^2, CI_i is the equivalent transfer coefficient of constructed land use of the *i*th wetland landscape, which is related to human activity intensities, n is the number of wetland landscape types in the region.

Spatial distribution of human activities

According to the analysis, the oil fields were the most disturbing areas of human activities from 1986 to 2016. After 2016, the development of salt fields and aqua-culture ponds in coastal areas are the region with great human disturbance.

The intensity of human activity has increased considerably over the past 40 years. In the study area, the largest disturbance of human activities is mainly concentrated in the coastal area. Human activities, such as oil field development, aqua-culture and salt industry, were greatly developed

Table 7 Area transfer in three modes and human activity impact index in 5 time periods

Time period	From natural To constructed and non-wetland	Ratio %	From constructed To non-wetland	Ratio %	From non-wetland To constructed	Ratio %	HAII %
1976–1986	250.84 km^2	96.09	0.21 km^2	0.08	10.01 km^2	3.83	16.77
1986–1996	274.75 km^2	83.36	23.34 km^2	7.08	31.52 km^2	9.56	23.89
1996–2006	311.66 km^2	87.20	18.25 km^2	5.11	27.51 km^2	7.70	32.60
2006–2016	500.0 km^2	62.92	24.51 km^2	3.08	270.15 km^2	34.0	52.94
1976–2016	1034.65 km^2	84.65	0.26 km^2	0.02	187.32 km^2	15.33	51.42

Note Ratio = Transferred area in different transfer modes /Total transferred area due to human activities

Table 8 The transferred proportion from natural wetland to different types of constructed wetland and non-wetland

Time period	Industrial	Dry land %	Architecture %	Ponds %	Forestry %	Paddy %	Salt land %	Aqua-Culture %	Garden %
1976–1986	10.94	66.54	3.50	0.80	6.78	9.61	0.64	1.19	0.00
1986–1996	7.94	56.85	1.63	8.96	7.14	4.18	1.39	11.91	0.00
1996–2006	10.28	44.44	0.60	12.87	3.07	2.73	19.98	5.64	0.40
2006–2016	1.81	15.57	9.12	33.80	4.14	11.22	11.07	13.28	0.00
1976–2016	7.56	23.67	4.66	22.05	6.17	17.20	7.29	10.83	0.57

within 40 years. The moderate human activities were mainly concentrated in the middle and lower part of the study area, which is related to the reclamation of dry fields and paddy fields. The establishment of nature reserve area plays an important role in wetland management.

Conclusion

This paper selected remote sensing images from Landsat and used the combination of CA-Markov and the MLP model to simulate the wetland landscape variation in the Yellow River Delta, the wetland landscape pattern and evolution has been obtained. The main research conclusions are as follows.

From 1976 to 2016, the wetland degradation trend was developed in the study area, and the total wetland area was decreased. The total area of wetland was decreased from 2594.76 km^2in 1976 to 2491.79 km^2in 2016. The natural wetland shows a downward decreasing trend, which has been decreased by 954.03 km^2. The constructed wetland shows an increasing trend. The area of the constructed wetland was increased by 851.06 km^2, in which paddy fields have been rapidly increased from 0 in 1976 to 333.25 km^2 in 2016.

During the dynamic evolution of wetland, the largest wetland transfer was happened in the natural wetland, in which 31.34% of suaeda glauca bunge were transferred to water ponds and 24.71% of reeds area were transferred to dry land. Some constructed wetlands were transferred to non-wetlands, in which 1.55% of water ponds were transferred to architecture land, 21.27% of constructed wetlands were transferred to dry land. With the increasing intensity of human activities, the landscape types in the study area are increasing. The number of patches, landscape diversity index, landscape evenness index and patch density show the increasing trend.

·The degradation of wetland in the Yellow River Delta is mainly affected by both natural and human activities, among which human intervention is the dominant factor. The human activity impact ratio has been reached 52.94% in 40 years, which is from 16.77% in the former 10 years to 52.94% in the latter 10 years. The natural wetland transfer caused by human activities was evenly distributed from 2006 to 2016, of which 34% were transferred to ponds. From 1976 to 2016, farmland reclamation was dominant component.

It can be seen from the simulation and predicted results in 2026 that the natural and non-wetland are reduced, the constructed wetland area is greatly increasing and expanding into shallow sea. In general, the wetland development in the Yellow River Delta shows the degraded trend, the natural wetland area is reduced, the overall connectivity between the wetland landscape patches is reduced, and the wetland in the Yellow River Delta is being evolved to the fragmented and complicated trend.

Acknowledgements The study was supported by the Natural Science Fund of China (No.50579020).

Author contribution The study conception and design, material preparation, data collection and analysis were performed by Ke ZHOU.

Funding The study was supported by the National Natural Science Fund of China (No.50579020).

Data Availability All the data and materials in the current study are available from the corresponding author on reasonable request.

Declarations

Conflict of interest There is no conflict of interest in this manuscript.

Consent for Publication All the data in the paper can be published without any competing financial interests or personal relationships that could have appeared to influence the work reported in this paper.

Ethical Approval The author consents to participate in the works under the Ethical Approval and Compliance with Ethical Standards.

References

Chang X, Zhang Q, Luo M (2014) Comparison of Qinzhou bay wetland landscape information extraction by three methods. Int Arch Photogramm Remote Sens Spat Inf Sci 40(3):21–28

Chen K (2019) Analysis on the evolving progress and driving force of estuarine wetland landscape types-- the yellow river delta wetland. Liaoning Norm Univ(D) 2019:8–49

Congru MU, Yang L, Jinghua WANG (2000) Formation and protection of wetland ecosystem in Yellow River Delta. J Appl Ecol 11(1):123–126

Davidson NC (2014) How much wetland has the world lost? Long-term and recent trends in global wetland area. Mar Freshw Res 65(10):934–941

Dong J, Xiao X, Menarguez MA (2016) Mapping paddy rice planting area in northeastern Asia with Landsat 8 images, phenology-based algorithm and Google Earth Engine. Remote Sens Environ 185:142–154

Dongying Municipal Government (2016).Dongying city "13th five-year plan "for modern agricultural development, Aug 2016

Dongying Municipal People's Government (2019) Dongying wetland conservation regulations(R), Feb 2019

Dronova I (2015) Object-based image analysis in wetland research: a review. Remote Sens 7(5):6380–6413

Escorihuel MJ, Quintana-Seguí P, Escorihuel MJ (2016) Comparison of remote sensing and simulated soil moisture datasets in Mediterranean landscapes. Remote Sens Environ 180:99–114

Frohn RC, Reif M, Lane C (2009) Satellite remote sensing of isolated wetlands using object-oriented classification of Landsat-7 data. Wetlands 29(3):931–941

Fu X, Liu G, Chai S (2013) Spatial-temporal analysis of wetland landscape pattern under the influence ofartificial dykes in the Yellow River delta. Chin J Population Resour Environ 11(2):109–117

Keddy PA (2000) Wetland ecology principles and conservation. Cambridge University Press, Cambridge, pp 124–238

Klemas V (2013) Using remote sensing to select and monitor wetland restoration sites: an overview. J Coast Res 29(4):958–970

Lin WANG, Xingwei CHEN (2007) Study on relationship between extracted river network and fractal dimension based on DEM. Geo Inf Sci 9(4):133–137

Liu Y, Wang G, Zhang F (2013) Spatial-temporal dynamic patterns of rural area development in eastern coastal China. Chin Geograph Sci 23(2):173–181

Liu J, Feng Q, Gong J (2016) Land-cover classification of the Yellow River Delta wetland based on multiple end-member spectral mixture analysis and a Random Forest classifier. Int J Remote Sens 37(8):1845–1867

Mao DH, Luo L, Wang ZM (2018) Conversions between natural wetlands and farmland in China: a multiscale geospatial analysis. Sci Total Environ 634:550–560

Mishra VN, Rai PK, Mohan K (2014) Prediction of land use changes based on land change modeler (LCM)using remote sensing: A case study of Muzaffarpur (Bihar), India. J Geograph Inst Jovan Cvijic Sasa 64(1):111–127

Mui A, He YH, Weng QH (2015) An object-based approach to delineate wetlands across landscapes of varied disturbance with high spatial resolution satellite imagery. ISPRS J PhotoGramm Remote Sens 109:30–46

Olmedo MTC, Pontius RGP, Paegelow M (2015) Comparison of simulation models in terms of quantity and allocation of land change. Environ Model Softw 69:214–221

Ozesmi SL, Bauer ME (2002) Satellite remote sensing of wetlands. Wetl Ecol Manag 10(5):381–402

Walter V (2004) Object-based classification of remote sensing data for change detection. ISPRS J Photogramm Remote Sens 58(3):225–238

Williams DC, Lyon JG (1995) Use of a geographic information system database to measure and evaluate wetland changes in the St. Mary's River. In: Wetland and environmental applications of GIS. CRC Press 35(2):125–140